BEAM POSITION FEEDBACK SYSTEM FOR THE ADVANCED PHOTON SOURCE*

Y. Chung
Argonne National Laboratory, Argonne, IL 60439

ABSTRACT

The Advanced Photon Source (APS) will implement both global and local beam position feedback systems to stabilize the particle and X-ray beams for the storage ring. The systems consist of 20 VME crates distributed around the ring, each running multiple digital signal processors (DSP) running at 4kHz sampling rate with a proportional, integral, and derivative (PID) control algorithm. The particle and X-ray beam position data is shared by the distributed processors through networked reflective memory. A theory of closed orbit correction using the technique of singular value decomposition (SVD) of the response matrix and simulation of its application to the APS storage ring will be discussed. This technique combines the global and local feedback systems and resolves the conflict among multiple local feedback systems due to local bump closure error. Maximum correction efficiency is achieved by feeding back the global orbit data to the local feedback systems. The effect of the vacuum chamber eddy current induced by the AC corrector magnet field for local feedback systems is compensated by digital filters. Results of experiments conducted on the X-ray ring of the National Synchrotron Light Source and the SPEAR at Stanford Synchrotron Radiation Laboratory will be presented.

INTRODUCTION

The third generation synchrotron light sources, of which the Advanced Photon Source (APS) is one, are characterized by low emittance of the charged particle beams and high brightness of the photon beams radiated from insertion devices. Transverse stability of the particle beams is a crucial element in achieving these goals and the APS will implement extensive beam position feedback systems, which include 320 corrector magnets, 360 positron beam position monitors (BPMs)

Table 1. Specifications of the beam position feedback systems.

	Global DC	Global AC	Local
Orbit measurement device	All of the RF BPMs	RF BPMs (1/sector)	RF BPMs X-ray BPMs
Correctors	All correctors (320)	Subset of correctors	Local bump
Specified orbit measurement resolution	25 μm	25 μm	1 μm
Achievable resolution	5 μm	5 μm	1 μm
Required range of correction	± 20 mm	± 500 μm	± 100 μm

*Work supported by the U.S. Department of Energy, Office of Basic Energy Sciences, under Contract No. W-31-109-ENG-38.

distributed around the storage ring of 1104 m circumference, miniature BPMs for insertion device beamlines, and photon beam position monitors in the front end of X-ray beamlines. The beam position feedback systems are largely divided into the global and local feedback systems according to the extent of correction, and the DC and AC feedback systems according to the bandwidth of correction.[1-4] Table 1 shows the specifications of the beam position feedback systems to be employed in the APS storage ring.

The APS beam position feedback system is characterized by: (1) digital implementation with proportional, integral, and derivative (PID) control, (2) an orbit correction algorithm based on singular value decomposition (SVD) of the response matrix, and (3) combination of the global and local feedback systems into a single, unified system for maximum correction efficiency and orbit stability.

DIGITAL SIGNAL PROCESSING

In order to avoid the problems characteristic of analog circuits, e.g., drift, offset, and sensitivity to temperature change, we will use digital signal processing (DSP) for beam position feedback. This also provides added flexibility through user programmability. The theory of digital signal processing is widely available in the literature[5-7], and will not be discussed in this paper.

In designing the digital signal processing scheme for closed loop feedback, the following factors must be considered: rise-time, overshoot, settling time, control effort, and noise throughput. The major parameters that determine the performance of the closed loop feedback are controller gains, open loop bandwidth, and sampling frequency.

For a simple digital closed-loop feedback system with the open-loop gain G, sampling frequency F_s, and open-loop bandwidth f_b with $F_s >> f_b$, it can be shown that the condition for critically damped response to a step impulse is

$$\frac{F_s}{G f_b} \approx 20. \qquad (1)$$

Since the bandwidth of the closed loop system is approximately equal to $G f_b$, the bandwidth of the optimally controlled feedback system is roughly equal to $F_s/20$.

Digital signal processing is also used in compensating for the effect of the eddy current induced in the relatively thick (1/2") aluminum vacuum chamber of the storage ring by the corrector magnets for the local beam position feedback systems. The global orbit feedback system uses a thin stainless steel chamber and is not significantly affected by the eddy current effect.

ORBIT CORRECTION ALGORITHM

The orbit correction algorithm for the beam position feedback systems is based on the analysis of the response matrix using the technique of singular value decomposition (SVD) of matrices.[8-13] SVD transforms the response matrix into a diagonal matrix, with the diagonal elements representing the correction efficiency of non-interacting orbit correction channels. The AC orbit correction is then equivalent to a combination of the DC correction algorithm and multiple non-interacting feedback systems.

Let us consider M BPMs and N correctors used for closed orbit correction in the storage ring. The i-th BPM has beta and phase functions (β_i, ψ_i), and similarly,

the j-th corrector has (β_{cj}, ψ_{cj}). The response matrix R_{ij} corresponding to the beam motion at the i-th BPM per unit angle of kick by the j-th corrector is then given by[14]

$$R_{ij} = \frac{\sqrt{\beta_i \beta_{cj}}}{2 \sin \pi\nu} \cos(|\psi_i - \psi_{cj}| - \pi\nu), \tag{2}$$

where ν is the betatron tune of the machine.

We write the response matrix $\mathbf{R}$ as a product of three matrices $\mathbf{U}$, $\mathbf{W}$, and $\mathbf{V}$ as[11]

$$\mathbf{R} = \mathbf{U} \cdot \mathbf{W} \cdot \mathbf{V}^T, \tag{3}$$

where $\mathbf{U}$ is an $M \times M$ unitary matrix ($\mathbf{U}^T \cdot \mathbf{U} = \mathbf{U} \cdot \mathbf{U}^T = \mathbf{1}$), $\mathbf{W}$ is an $M \times N$ diagonal matrix with positive or zero elements, and $\mathbf{V}$ is an $N \times N$ unitary matrix ($\mathbf{V}^T \cdot \mathbf{V} = \mathbf{V} \cdot \mathbf{V}^T = \mathbf{1}$). This decomposition is unique only to a certain extent, and there are other ways of decomposing the matrix $\mathbf{R}$.[15,16]

Let us denote by Δx the global orbit change due to the corrector strength change $\Delta\boldsymbol{\theta}$ and define

$$\Delta \mathbf{x}^t = \mathbf{U}^T \cdot \Delta \mathbf{x} \quad \text{and} \quad \Delta \boldsymbol{\theta}^t = \mathbf{V}^T \cdot \Delta \boldsymbol{\theta}. \tag{4}$$

Then, from Eqs. (3) and (4) we have

$$\Delta \mathbf{x}^t = \mathbf{W} \cdot \Delta \boldsymbol{\theta}^t. \tag{5}$$

Equation (4) is the rule of transformation for the BPMs and correctors. $\Delta \mathbf{x}^t$ and $\Delta \boldsymbol{\theta}^t$ are the vectors in the transformed BPM (t-BPM) space and transformed corrector (t-corrector) space, respectively. The columns of the matrices $\mathbf{U}$ and $\mathbf{V}$ are the orthogonal basis vectors $\{\mathbf{u}_i\}$ and $\{\mathbf{v}_j\}$. The elements of the matrix $\mathbf{W}$ are given by

$$W_{ij} = w_{\min(i,j)} \delta_{ij}. \tag{6}$$

We call these diagonal elements w_n (≥ 0, $1 \leq n \leq \min(M, N)$) eigenvalues, which represent the coupling efficiency between the t-BPMs and t-correctors. The matrix $\mathbf{R}$ is singular if any of the eigenvalues are equal to zero. The basis vectors are related through the relation

$$\mathbf{R} \cdot \mathbf{v}_n = w_n \mathbf{u}_n. \qquad 1 \leq n \leq \min(M, N) \tag{7}$$

The response matrix for the t-BPMs and t-correctors, $\mathbf{W}$, is diagonal in Eq. (5), and therefore, analysis of orbit correction is straightforward in the transformed spaces. Results for real BPMs and correctors can be obtained by inverse transformation. Since the transformation is orthogonal, the r.m.s. orbit error and the overall corrector strength are conserved. When the number of correctors is larger than the number of coupled channels, the decoupled t-correctors can be used to further optimize the correctors.

GLOBAL ORBIT FEEDBACK

In this section, we will discuss application of the SVD algorithm to global orbit feedback on the National Synchrotron Light Source (NSLS) for DC and on SPEAR at Stanford Synchrotron Radiation Laboratory (SSRL). Analysis of the global orbit feedback on the APS storage ring will also be discussed.

A. Experiments on the NSLS X-ray Ring and SPEAR, SSRL[17]

For the NSLS X-ray ring, all of the 48 (M) BPMs and 39 (N) correctors available for orbit correction were used. Figure 1(a) shows the result of orbit

correction using 35 eigenvalues, where the initial r.m.s. orbit error of 138 μm was reduced to 61 μm. Similar reduction of absolute orbit error from 780 μm to 215 μm in SPEAR at SSRL is shown in Fig. 1(b), where 17 BPMs and 30 correctors were used with 15 eigenvalues.

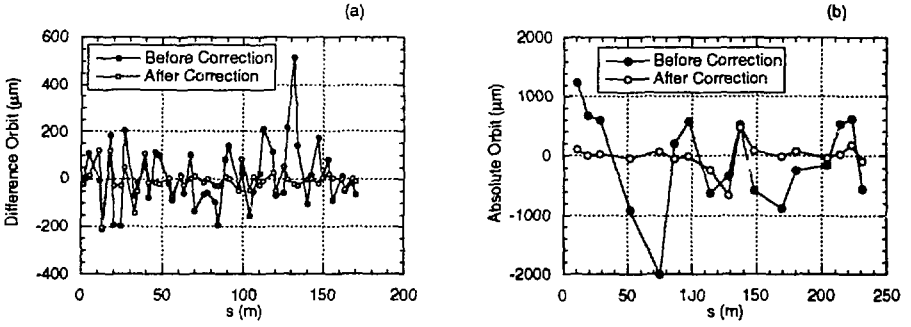

Fig. 1: DC global orbit correction on (a) the NSLS X-ray ring and (b) SPEAR, SSRL.

Figure 2 shows the result of global AC beam position feedback experiments conducted on SPEAR at SSRL. Ten BPMs were used to detect beam motion and 16 correctors were used for closed orbit correction. The sampling frequency was 37 Hz and the open loop bandwidth was set at 1% of the sampling frequency, that is, 0.37 Hz. Since the proportional gain K_P is 3, closed loop bandwidth of approximately 1 Hz can be expected, which is in good agreement with the result shown in Fig. 2(b). This implies that the orbit correction bandwidth for the APS with 4-kHz sampling frequency will be approximately 100 Hz.

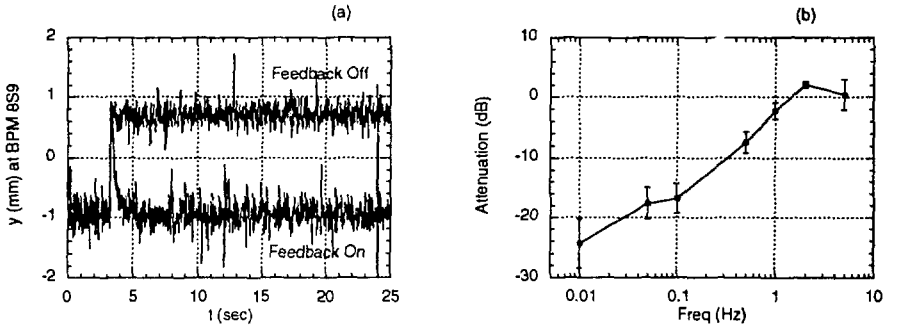

Fig. 2: Result of global orbit feedback on SPEAR, SSRL in (a) time domain and (b) frequency domain. The parameters used were: $K_P = 3$, $K_I = 0.05$, $K_D = 0$, $F_s = 37$ Hz, and $f_b = 0.37$ Hz.

B. Analysis of the APS Storage Ring

The APS storage ring has 40 sectors and each has nine BPMs (total 360) and eight correctors (total 320) available for global orbit correction. The distribution of BPMs and correctors is identical for all sectors. Figure 3(a) shows the eigenvalues w_n ($1 \le n \le 320$) in descending order when all BPMs and correctors are used. The

maximum and minimum values are 1.140×10^{3} and 9.126×10^{-2} in units of m/rad, respectively. The large decrease at n = 240 indicates that 80 of the correctors are almost redundant and therefore do not contribute much to orbit correction except to reduce overall corrector strengths. Figure 3(b) shows the plot of the BPM basis vectors U_{i1} and U_{i2} as functions of the BPM index i, which correspond to the largest eigenvalues w_1 and w_2.

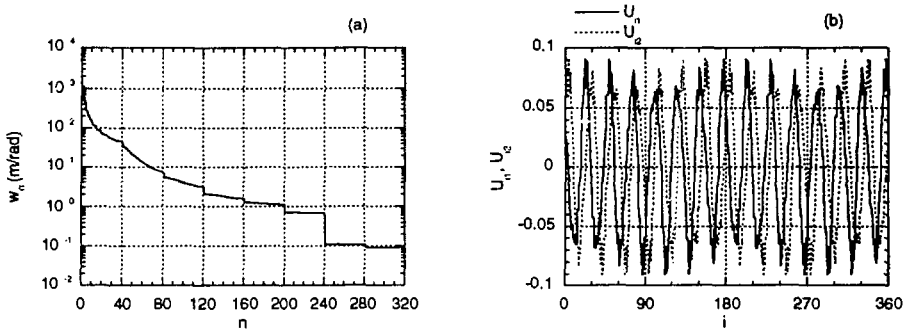

Fig. 3: (a) Plot of the eigenvalues in descending order for the APS storage ring with M = 360 and N = 320 in the vertical plane and (b) the BPM basis vectors U_{i1} and U_{i2} ($1 \le i \le 360$) for the most strongly coupled channels.

For global AC feedback, the same number (M = N = 40) of BPMs and correctors are used for both the horizontal and vertical planes. The BPMs and correctors are located an equal distance apart around the 40 sectors. As a result, correspondence exists between the SVD eigenmodes and harmonic modes, as is shown in Fig. 4. The ten largest SVD eigenvalues were used for orbit correction in the horizontal plane and noise attenuation for (a) SVD eigenmodes and (b) harmonic modes was calculated. With the betatron tune $\nu_H = 35.2154$, the harmonic modes m = 5 and 35 correspond to the largest eigenvalues $w_{1,2} = 181$ m/rad. Similar correspondence can be found for other modes.

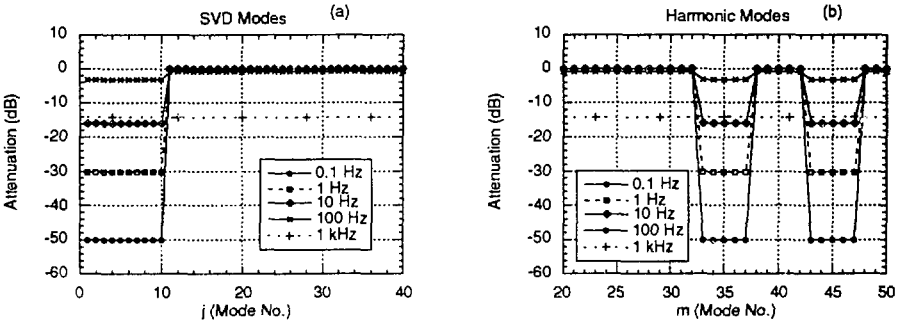

Fig. 4: Correspondence between the (a) SVD eigenmodes and (b) harmonic modes for global AC feedback in the horizontal plane of the APS storage ring. The ten largest SVD eigenvalues are used for orbit correction in the horizontal plane.

LOCAL ORBIT FEEDBACK

The local feedback systems primarily handle isolated noise on the X-ray beamline and will employ four-magnet bumps to control both the position and the angle of the X-ray source point as shown in Fig. 5. For the bending magnet radiation, the source point is placed at the center of the main dipole, while for the insertion device, the radiation is along the extension of the line adjoining the beam position at the location of bump magnets 2 and 3.

Even though the local bump as shown in Fig. 5 is designed to be truly local and not perturb other local systems or the global system, bump coefficient error, magnet field error, and eddy current effect can cause local bump closure error and thus global orbit perturbation. For multiple such local feedback systems, the resulting cross-talk among them can lead to oscillation and instability. Even though this effect can be partially canceled by the global feedback system, it will unnecessarily perturb the local orbits as well. As a result, the orbit correction efficiency will decrease.

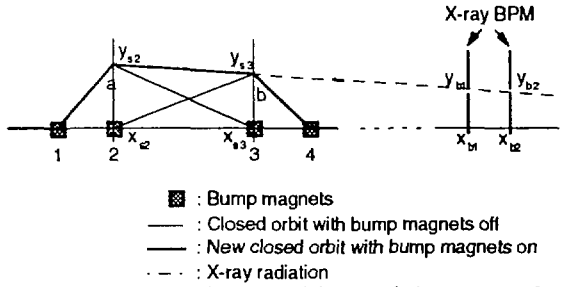

Fig. 5: Four-magnet bump to control the position and the angle of the X-ray radiation, which comprises two three-magnet bumps a (magnets 1, 2, and 3) and b (magnets 2, 3, and 4).

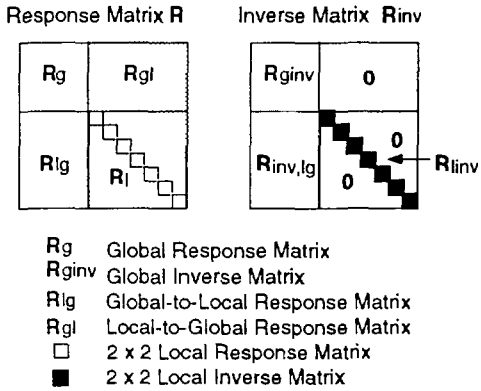

Fig. 6: Response matrix and its inverse for the unified feedback system.

One can find a way to resolve this by considering the global and local feedback systems as a single, unified feedback system. Consider the full response matrix **R** and its inverse as shown in Fig. 6. For the case of no local bump closure error, we will have the local-to-global matrix $\mathbf{R}_{gl} = \mathbf{0}$. In general, the global-to-local matrix $\mathbf{R}_{lg}$

is not zero. For independent operation of the global and local feedback systems, the off-diagonal matrix $\mathbf{R}_{inv,lg}$ is equal to zero, and it can be easily seen that $\mathbf{R}\cdot\mathbf{R}_{inv}$ has off-diagonal elements which represent the global-to-local interaction. This unidirectional interaction is canceled out by putting

$$\mathbf{R}_{inv,lg} = -\mathbf{R}_{linv}\cdot\mathbf{R}_{lg}\cdot\mathbf{R}_{ginv}. \tag{8}$$

The physical interpretation of Eq. (8) can be given as follows. $\mathbf{R}_{ginv}$ is the response of the global correctors to global orbit perturbation, $\mathbf{R}_{lg}$ is the local orbit perturbation due to global correctors, and $\mathbf{R}_{linv}$ is the response of the local correctors to local orbit perturbation. The matrix product $\mathbf{R}_{linv}\cdot\mathbf{R}_{lg}\cdot\mathbf{R}_{ginv}$ is then the response of the local correctors to global orbit perturbation and $\mathbf{R}_{inv,lg}$ in Eq. (8) compensates for the action of the global feedback system on the local orbits, resulting in maximum orbit correction efficiency. Figure 7 shows improvement of local orbit correction efficiency when the global and local feedback systems are unified. The noise sources are SVD eigenmodes. Random field error less than 2% and orbit deviation less than 3 mm were assumed with the vacuum chamber eddy current taken into account.

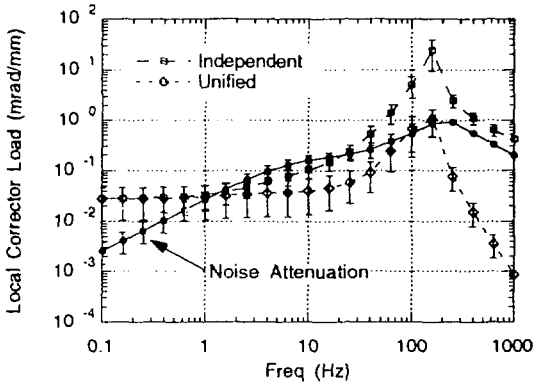

Fig. 7: Improvement of local orbit correction efficiency for the unified system. The noise sources are SVD eigenmodes. Random field error less than 2% and orbit deviation less than 3 mm were assumed with the vacuum chamber eddy current taken into account.

SUMMARY

The design principle of the APS beam position feedback system consists of an orbit correction algorithm based on singular value decomposition (SVD) of the response matrix and digital signal processing (DSP) with a proportional, integral, and derivative (PID) control algorithm. SVD transforms the response matrix such that the matrix product of the machine response and its inverse for orbit correction becomes a diagonal matrix. This renders the feedback system into multiple non-interacting closed loop feedback systems, to which we can apply the theory of single-channel digital feedback. These basic design concepts were verified through experiments on the NSLS X-ray ring and SPEAR at SSRL.

As a departure from the conventional approach to beam position feedback, the global and local feedback systems are combined into a single, unified feedback system. The effect of local bump closure error in the local systems is reduced through

orbit correction by the global feedback system. This approach removes the undesirable interaction between the global and local feedback systems and maximizes orbit correction efficiency.

ACKNOWLEDGMENTS

The author would like to thank G. Decker, L. Emery, K. Evans, Jr., J. Kirchman, F. Lenkszus, and A. J. Votaw of the APS project for their contributions to this work. Thanks also go to J. Galayda, M. Knott, A. Lumpkin, and L. Teng for their support and interest. J. Safranek, I. So, and Y. Tang at NSLS and R. Hettel, W. J. Corbett, M. Lee, J. Sebek, and J. Yang at SSRL are to be thanked for their collaboration on the measurements.

REFERENCES

1. R. O. Hettel, "Beam Steering at the Stanford Synchrotron Radiation Laboratory," IEEE Trans. Nucl. Sci., **NS-30**, No. 4, p. 2228, 1983.
2. R. J. Nawrocky et al., "Automatic Beam Steering in the NSLS Storage Rings Using Closed Orbit Feedback," Nucl. Instr. and Meth., **A266**, p. 164, 1988.
3. L. H. Yu et al., "Real Time Closed Orbit Correction System," *Proceedings of IEEE Particle Accelerator Conference*, Chicago, 1989.
4. D. Bulfone et al., "Design Considerations for the Elettra Beam Position Feedback Systems," *Proceedings of the 2nd European Particle Accelerator Conference*, Nice, 1990.
5. Y. Chung, L. Emery, and J. Kirchman, "Compensation for the Effect of Vacuum Chamber Eddy Current by Digital Signal Processing for Closed Orbit Feedback," *Proceedings of IEEE Particle Accelerator Conference*, Washington, D.C., 1993.
6. A. Peled and B. Liu, *Digital Signal Processing*, John Wiley & Sons, 1976.
7. Y. Chung, L. Emery, and K. Kirchman, "Digital Signal Processing for Beam Position Feedback," LS Note 202, ANL, 1992.
8. G. H. Golub and C. Reinsch, "Singular Value Decomposition and Least Squares Solutions," Numer. Math. **14**, pp. 403–420, 1970, and references therein.
9. G. E. Forsythe, M. A. Malcolm, and C. B. Moler, *Computer Methods for Mathematical Computations*, Prentice-Hall, Englewood Cliffs, N.J., 1977.
10. J. J. Dongarra, et al., *LINPACK User's Guide*, Chapter 11, Society for Industrial and Applied Mathematics, Philadelphia, 1979.
11. *MATLAB™ User's Guide*, The Mathworks, Inc., p. 3-178, 1990.
12. K. J. Kleman, "Beam Diagnostics and Control at Aladdin," Nuclear Inst. and Meth., **A266**, p. 172, 1988.
13. Y. Chung, G. Decker, and K. Evans, Jr., "Closed Orbit Correction Using Singular Value Decomposition of the Response Matrix," *Proceedings of IEEE Particle Accelerator Conference*, Washington, D.C., 1993.
14. M. Sands, "The Physics of Electron Storage Rings - An Introduction," SLAC-121, 1970.
15. W. Press et al., *Numerical Recipes in C*, Cambridge University Press, p. 60, 1989.
16. *Mathematica™*, Wolfram Research, Inc., p. 454, 1988.
17. Y. Chung, et al., "Global DC Closed Orbit Correction Experiments on the NSLS X-ray Ring and SPEAR," *Proceedings of IEEE Particle Accelerator Conference*, Washington, D.C., 1993.